

Third SPE Comparative Solution Project: Gas Cycling of Retrograde Condensate Reservoirs

Douglas E. Kenyon, SPE, Marathon Oil Co.
G. Alda Behie, SPE, Dynamic Reservoir Systems

Summary. Nine companies participated in this artificial modeling study of gas cycling in a rich retrograde-gas-condensate reservoir. Surface oil rate predictions differ in the early years of cycling but agree better late in cycling. The amount of condensate precipitated near the production well and its rate of evaporation varied widely among participants. The explanation appears to be in K -value techniques used. Precomputed tables for K values produced rapid and thorough removal of condensate during later years of cycling. Equation-of-state (EOS) methods produced a stabilized condensate saturation sufficient to flow liquid during the greater part of cycling, and the condensate never completely revaporized. We do not know which prediction is more nearly correct because our PVT data did not cover the range of compositions that exists in this area of the reservoir model.

Introduction

SPE conducted two earlier solution projects,^{1,2} both designed to measure the state-of-the-art simulation capability for challenging and timely modeling problems. The first project involved a three-layer black-oil simulation with gas injection into the top layer.¹ Both constant and variable bubblepoint pressure assumptions were used. Model predictions were in fair agreement. No simulator performance data (run times, timestep size, etc.) were given. Seven companies participated in the project. The second project was a study of water and gas coning with a radial grid and 15 layers.² Authors of the project felt that unusual well rate variations and a high assumed solution GOR contributed to the difficulty of the problem. Some significant discrepancies in oil rate and pressure were obtained. Eleven companies joined in the project.

For the third comparative solution project, the Committee for the Numerical Simulation Symposium sought a compositional modeling problem. Numerical comparisons of the PVT data match were considered important. Speed of the simulators was not to be of major interest.

The problem we designed is the outcome of this fairly general request. Some features of interest in current production practice of pressure maintenance by gas injection are included. The results confirm the well-known trade-off between the timing of gas sales and the amount of condensate recovered. Several features of interest in a more complete examination of production from gas-condensate reservoirs are ignored. These include the effects of near-well liquid saturation buildup on well productivity and of water encroachment and water production on hydrocarbon productivity. We did not address the role of numerical dispersion. In addition, the surface process is simplified and not representative of economical liquid recovery in typical offshore operations. We simplified the surface process to attract a larger number of participants

because not all companies had facilities for simulating gas plant processing with gas recycling in their compositional simulators.

Nine companies responded to the invitation for participation. Table 1 is a list of the participants in this project. Participant responses were well prepared and required a minimum of discussion. We invited all the companies to use as many components as necessary for the accurate match of the PVT data and for the simulation of gas cycling. Companies were asked to give components actually used in the reservoir model, how these components were characterized, and the match to the PVT data obtained with the components.

We first outline the problem specifications, including sufficient data for others who may wish to try the problem. The pertinent PVT data are given. We show each participant's components, the properties of these components, and the basic PVT match obtained. In many cases, EOS methods were used exclusively, but in others, a combination of methods was applied. The results of the reservoir simulation are given and comparisons are shown between companies for both cycling-strategy cases. Finally, some facts regarding simulator performance are given, although this information was voluntary.

Problem Statement

The two major parts to a compositional model study are the PVT data and the reservoir grid. For the PVT data, participants were supplied with a companion set of fluid analysis reports. The specification of the reservoir model is given in Tables 2 and 3 and the grid is shown in Fig. 1. Note that the grid is $9 \times 9 \times 4$ and symmetrical, indicating that it would be possible to simulate half the indicated grid. Most participants chose to model the full grid. Note also that the layers are homogeneous and of constant porosity, but that permeability and thickness vary among layers.

TABLE 1—COMPANIES PARTICIPATING IN THIRD SPE COMPARATIVE SOLUTION PROJECT

Arco Oil and Gas Co.
P.O. Box 2819
Dallas, TX 75221

Chevron Oil Field Research Co.
P.O. Box 446
La Habra, CA 90631

Core Laboratories Inc.
7600 Carpenter Freeway
P.O. Box 47547
Dallas, TX 75247

Computer Modelling Group (CMG)
3512-33 Street N.W.
Calgary, Alta.
Canada T2L 2A6

Soc. Natl. Elf Aquitaine
26, Avenue des Lilas
64018 Pau Cedex
France

Intercomp*
1801 California St.
Fourth Floor
Denver, CO 80202-2699

Marathon Oil Co.
P.O. Box 269
Littleton, CO 80160-0269

McCord-Lewis Energy Services
P.O. Box 45307
Dallas, TX 75245

Petek, The Petroleum Technology Research Inst.
N-7034 Trondheim NTH
Norway

*Now Scientific Software-Intercomp.

TABLE 2—RESERVOIR GRID AND SATURATION INPUT DATA

Reservoir Grid Data

NX = NY = 9, NZ = 4
DX = DY = 293.3 ft
Datum (subsurface), ft 7,500
Porosity (at initial reservoir pressure) 0.13
Gas/water contact, ft 7,500
Water saturation at contact 1.00
Capillary pressure at contact, psi 0
Initial pressure at contact, psia 3,550
Water properties
density at contact, lbm/ft³ 63.0
compressibility, psi⁻¹ 3.0 × 10⁻⁶
PV compressibility, psi⁻¹ 4.0 × 10⁻⁶

Layer	Horizontal Permeability	Vertical Permeability	Thickness (ft)	Depth to Center (ft)
1	130	13	30	7,330
2	40	4	30	7,360
3	20	2	50	7,400
4	150	15	50	7,450

Saturation Data

Phase Saturation	k_{rg}	k_{ro}	k_{rw}	Gas/Water Capillary Pressure (psi)
0.00	0.00	0.00	0.00	> 50
0.04	0.005	0.00	0.00	> 50
0.08	0.013	0.00	0.00	> 50
0.12	0.026	0.00	0.00	> 50
0.16	0.040	0.00	0.00	50
0.20	0.058	0.00	0.002	32
0.24	0.078	0.00	0.010	21
0.28	0.100	0.005	0.020	15.5
0.32	0.126	0.012	0.033	12.0
0.36	0.156	0.024	0.049	9.2
0.40	0.187	0.040	0.066	7.0
0.44	0.222	0.060	0.090	5.3
0.48	0.260	0.082	0.119	4.2
0.52	0.300	0.112	0.150	3.4
0.56	0.348	0.150	0.186	2.7
0.60	0.400	0.196	0.227	2.1
0.64	0.450	0.250	0.277	1.7
0.68	0.505	0.315	0.330	1.3
0.72	0.562	0.400	0.390	1.0
0.76	0.620	0.513	0.462	0.7
0.80	0.680	0.650	0.540	0.5
0.84	0.740	0.800	0.620	0.4
0.88			0.710	0.3
0.92			0.800	0.2
0.96			0.900	0.1
1.00			1.000	0.0

Capillary pressure for gas/oil is assumed to be zero.

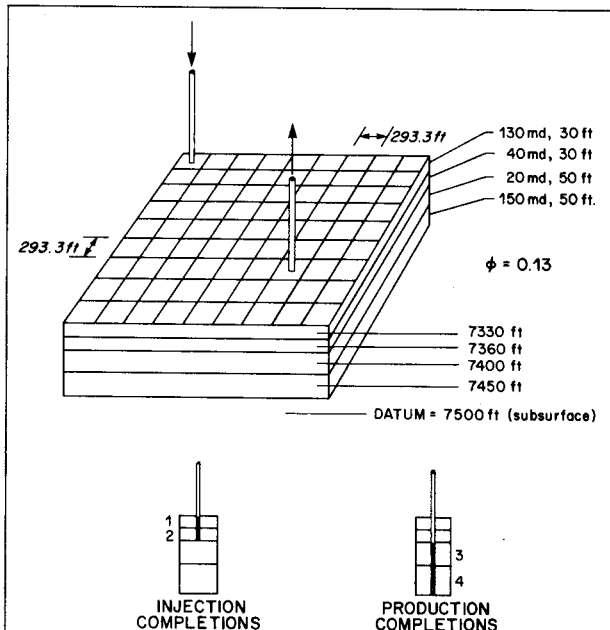


Fig. 1—Third comparative solution project 9 × 9 × 4 reservoir model grid.

The grid size sets the value of numerical dispersion in these implicit pressure, explicit saturation (IMPES) models. The grid size selected represents a reasonable grid for certain offshore applications but is somewhat too refined for a full-field simulation. The producer is not in the very corner of the grid. Most of the area behind the producer undergoes pressure depletion only because it is not swept by injection gas. In this area, retrograde condensation occurs without significant evaporation by recycle gas to simulate areas of minimal sweep in a real reservoir.

The initial conditions for the location of the gas/water contact and the capillary pressure data generate a water/gas transition zone extending into the pay layers. The very small compressibility and volume of water, however,

make water rather insignificant for this problem. Relative permeability data were based on the simplistic assumption that the relative permeability of any phase depends only on its saturation. Note that condensate is immobile up to 24% saturation and that k_{rg} is reduced from 0.74 to 0.40 as condensate builds to this saturation with irreducible water present.

Layer 1 is a high-permeability layer (130 md) with rapid movement of injected gas. The produced gas becomes a mix of reservoir gas with "dry gas." The path of migration of injected gas is along Layer 1 with a turn downward only in a small zone around the producer, which is completed in Layers 3 and 4. Layer 4 is also a high-permeability layer (150 md), but our review of saturation array data revealed that most of the injected gas that reaches the producer in Layer 4 has come across Layer 1 and turned downward as it approaches the producer. We speculate that buoyancy, high vertical permeability, and some extra water in Layer 4 explain the favored flow of dry gas through Layer 1.

Liquid production by multistage separation is the unknown to be predicted. The primary separator pressure depends on reservoir pressure as given in Table 3. Production is controlled by a specified separator-gas rate. Injected gas is taken from the combined vapor streams of the three-stage separation. Two cases were requested and differ by the recycle-gas rate assumed. Volumetrically, the two cases provide for exactly the same amount of recycle gas to be injected over the duration of the cycling period (10 years). Case 1 uses a constant recycle-gas rate (4,700 Mscf/D [133×10^3 std m^3/d]) for the entire cycling period. Case 2 uses a somewhat higher rate (5,700 Mscf/D [161×10^3 std m^3/d]) for the first 5 years of cycling and a somewhat lower rate (3,700 Mscf/D [105×10^3 std m^3/d]) for the last 5 years of cycling. More gas is recycled in the critical early years in Case 2. This promotes pressure maintenance and increases surface liquid yield (less condensation in the reservoir) but

TABLE 3—WELL AND SEPARATOR INPUT DATA

Production, Injection, and Sales Data		
Production Well Data		
Location $I=J=7$		
Perforations $K=3, 4$ (bottom layers)		
Radius, r_w , ft		1
Rate (separator gas rate), Mscf/D		6,200
Minimum bottomhole pressure, psi		500
Injection Well Data		
Location $I=J=1$		
Perforations $K=1, 2$ (top layers)		
Radius, r_w , ft		1
Rate (separator-gas rate minus sales-gas rate)		4,000
Maximum bottomhole pressure, psi		4,000
Sales Rate		
Case 1 (constant sales rate to blowdown)		
0 < t < 10 years: 1,500 Mscf/D		
t > 10 years: all produced gas to sales		
Case 2 (deferred sales)		
0 < t < 5 years: 500 Mscf/D		
5 < t < 10 years: 2,500 Mscf/D		
t > 10 years: all produced gas to sales		
Separator Pressures and Temperatures		
Separator	Pressure (psia)	Temperature (°F)
Primary*	815	80
Primary*	315	80
Second stage	65	80
Stock tank	14.7	60

* Primary separator at 815 psia until reservoir pressure (at datum) falls below 2,500 psia, then switch to primary separator at 315 psia.

reduces available sales gas volume. Reservoir pressure falls rapidly during the last years of cycling in Case 2 and surface liquid falls accordingly.

Blowdown (all gas to sales) starts at the end of the 10th year of cycling, and the models were run to 15 years or 1,000-psi [6.9-MPa] average reservoir pressure, which-

TABLE 4—HYDROCARBON ANALYSES OF SEPARATOR PRODUCTS AND CALCULATED WELL STREAM

Component	Separator Liquid (mol %)	Separator Gas*		Well Stream	
		(mol %)	(gal/scf × 10 ³)	(mol %)	(gal/scf × 10 ³)
Carbon dioxide	0.39	1.39		1.21	
Nitrogen	0.23	2.33		1.94	
Methane	12.55	78.03		65.99	
Ethane	6.71	9.13		8.69	
Propane	10.04	4.98	1.363	5.91	1.617
Isobutane	6.34	1.50	0.488	2.39	0.777
n-Butane	8.37	1.52	0.476	2.78	0.871
Isopentane	6.21	0.52	0.189	1.57	0.571
n-Pentane	4.63	0.33	0.119	1.12	0.403
Hexanes	8.67	0.27	0.110	1.81	0.734
Heptanes plus	35.86	nil	nil	6.59	3.756
Total	100.00	100.00	2.745	100.00	8.729
Properties of heptanes plus					
API gravity at 60°F	51.4				
Specific gravity at 60/60°F	0.7737			0.774	
Molecular weight	140			140	
Calculated separator-gas gravity (air = 1.000) = 0.736					
Calculated gross heating value for separator gas = 1,216 Btu/ft ³ of dry gas at 14.65 psia and 60°F					
Primary separator-gas/separator-liquid ratio 4,812 scf/bbl at 72°F, 2,000 psia					

* Gas synthetically prepared in the laboratory, liquid is random condensate sample; gas and liquid not in equilibrium at 2,000 psia.

TABLE 5—HYDROCARBON ANALYSIS OF RESERVOIR FLUID SAMPLE

Component	Mol %
Carbon dioxide	1.21
Nitrogen	1.94
Methane	65.99
Ethane	8.69
Propane	5.91
Isobutane	2.39
n-Butane	2.78
Isopentane	1.57
n-Pentane	1.12
Hexanes	1.81
Heptanes	1.44
Octanes	1.50
Nonanes	1.05
Decanes	0.73
Undecanes	0.49
Dodecanes	0.34
Tridecanes	0.26
Tetradecanes	0.20
Pentadecanes	0.13
Hexadecanes	0.11
Heptadecanes	0.08
Octadecanes	0.06
Nonadecanes	0.05
Eicosanes plus*	0.15
Total	100.00

*Assumed molecular weight = 325.

TABLE 6—PRESSURE/VOLUME RELATIONS OF RESERVOIR FLUID AT 200°F (Constant-Composition Expansion)

Pressure (psig)	Relative Volume	Deviation Factor, Z
6,000	0.8045	1.129
5,500	0.8268	1.063
5,000	0.8530	0.998
4,500	0.8856	0.933
4,000	0.9284	0.869
3,600	0.9745	0.822
3,428	1.0000	0.803* (dewpoint)
3,400	1.0043	
3,350	1.0142	
3,200	1.0468	
3,000	1.0997	
2,800	1.1644	
2,400	1.3412	
2,000	1.6113	
1,600	2.0412	
1,300	2.5542	
1,030	3.2925	
836	4.1393	

*Gas expansion factor = 1.295 Mscf/bbl.

ever occurred first. Models were initialized at pressures about 100 psi [690 kPa] above the dewpoint pressure of 3,443 psia [24 MPa].

PVT Data

Measured PVT data are given in Tables 4 through 15. The data include hydrocarbon sample analyses, constant-composition expansion data, constant-volume depletion data, and swelling data of four mixtures of reservoir gas with lean gas.

Table 4 gives compositions of liquid and gas used to create a reservoir well-stream composition for depletion

TABLE 7—RETROGRADE CONDENSATION DURING GAS DEPLETION AT 200°F (Constant-Volume Depletion)

Pressure (psig)	Retrograde Liquid Volume (% hydrocarbon pore space)
3,428	0.0
3,400	0.9
3,350	2.7
3,200	8.1
3,000*	15.0*
2,400	19.9
1,800	19.2
1,200	17.1
700	15.2
0	10.2

*First depletion level.

and swelling tests. Unlike most fluid analyses, the separator-gas composition was prepared in the laboratory with pure components and not collected in the field. Furthermore, the separator liquid is a random condensate sample. These fluids were physically recombined at a gas/liquid ratio of 4,812 scf/STB [857 std m³/stock-tank m³]. The resultant well-stream composition is correctly given in Table 4. Because gas and liquid samples used for recombination are not in equilibrium, however, the well stream will not flash to the gas and liquid compositions of Table 4 at the indicated pressure and temperature. This peculiarity was spelled out in the cover letter of the fluid-analysis report sent to all potential participants.

Table 5 gives more detail on the distribution of components in the synthetic reservoir fluid. However, none of the companies used this many components for the PVT match.

Table 6 gives constant-composition expansion data, including calculated Z factors at and above the dewpoint pressure. We will see later that all companies matched the relative volume in expansion accurately but that there were some minor differences in calculated Z factors.

Retrograde condensate observed during constant-volume depletion of the original mixture is shown in Table 7. Compositions of equilibrium gas are given in Table 8, and the calculated yields of separator and gas-plant products are given in Table 9. Most participants chose to use these data to match surface volumes produced by reservoir gas processed in the multistage separators. At least one participant chose to predict surface volumes without recourse to the data in Table 9 because such data are calculated, not measured.

Swelling tests with the reservoir gas and a synthetically prepared lean gas were performed. The lean-gas composition is given in Table 10. Note that the lean gas is virtually free from C₃₊ fractions. This contrasts with the separator gas used as recycle gas in the reservoir problem, which has approximately 10% C₃₊. Thus the relevance of matching the swelling data is in question for the problem at hand. Because participants matched the swelling data for the lean gas (with varied success), however, the less severe swelling and dewpoint pressure excursions in the reservoir model should be adequately covered.

Tables 11 through 15 give pressure/volume data for expansions at 200°F [93°C] for four mixtures of lean gas with reservoir gas. Liquid condensation data are given for each of the expansions. The reservoir model operates

TABLE 8—DEPLETION STUDY AT 200°F

Component	Hydrocarbon Analyses of Produced Well Stream (mol %)						
	Reservoir Pressure (psig)						
	3,428	3,000	2,400	1,800	1,200	700	700*
Carbon dioxide	1.21	1.24	1.27	1.31	1.33	1.32	0.44
Nitrogen	1.94	2.13	2.24	2.27	2.20	2.03	0.14
Methane	65.99	69.78	72.72	73.98	73.68	71.36	12.80
Ethane	8.69	8.66	8.63	8.79	9.12	9.66	5.27
Propane	5.91	5.67	5.46	5.38	5.61	6.27	7.12
Isobutane	2.39	2.20	2.01	1.93	2.01	2.40	4.44
n-Butane	2.78	2.54	2.31	2.18	2.27	2.60	5.96
Isopentane	1.57	1.39	1.20	1.09	1.09	1.23	4.76
n-Pentane	1.12	0.96	0.82	0.73	0.72	0.84	3.74
Hexanes	1.81	1.43	1.08	0.88	0.83	1.02	8.46
Heptanes	1.44	1.06	0.73	0.55	0.49	0.60	8.09
Octanes	1.50	1.06	0.66	0.44	0.34	0.40	9.72
Nonanes	1.05	0.69	0.40	0.25	0.18	0.16	7.46
Decanes	0.73	0.43	0.22	0.12	0.08	0.07	5.58
Undecanes	0.49	0.26	0.12	0.06	0.03	0.02	3.96
Dodecanes plus	1.38	0.50	0.13	0.04	0.02	0.02	12.06
Total	100.00	100.00	100.00	100.00	100.00	100.00	100.00
Molecular weight of heptanes plus	140	127	118	111	106	105	148
Specific gravity of heptanes plus	0.774	0.761	0.752	0.745	0.740	0.739	0.781
Deviation factor, Z							
Equilibrium gas	0.803	0.798	0.802	0.830	0.877	0.924	
Two-phase flow	0.803	0.774	0.748	0.730	0.703	0.642	
Cumulative initial well stream produced (%)	0.000	9.095	24.702	42.026	59.687	74.019	
Gal/scf × 10 ³ from smooth compositions							
Propane plus	8.729	6.598	5.159	4.485	4.407	5.043	
Butanes plus	7.112	5.046	3.665	3.013	2.872	3.328	
Pentanes plus	5.464	3.535	2.287	1.702	1.507	1.732	

*Equilibrium liquid phase representing 10.762% of original well stream.

TABLE 9—CALCULATED CUMULATIVE RECOVERY DURING DEPLETION*

	Initial	Reservoir Pressure (psig)					
		3,428	3,000	2,400	1,800	1,200	700
Well stream, Mscf	1,000	0	90.95	247.02	420.26	596.87	740.19
Normal temperature separation**							
Stock-tank liquid, bbl	131.00	0	7.35	14.83	20.43	25.14	29.25
Primary separator gas, Mscf	750.46	0	74.75	211.89	369.22	530.64	666.19
Second-stage gas, Mscf	107.05	0	7.25	16.07	23.76	31.45	32.92
Stock-tank gas, Mscf	27.25	0	2.02	4.70	7.15	9.69	11.67
Total plant products in primary-separator gas, gal							
Propane	801	0	85	249	443	654	876
Butanes (total)	492	0	54	163	295	440	617
Pentanes plus	206	0	22	67	120	176	255
Total plant products in second-stage gas, gal							
Propane	496	0	35	80	119	161	168
Butanes (total)	394	0	30	69	106	146	153
Pentanes plus	164	0	12	29	45	62	65
Total plant products in well stream, gal							
Propane	1,617	0	141	374	629	900	1,146
Butanes (total)	1,648	0	137	352	580	821	1,049
Pentanes plus	5,464	0	321	678	973	1,240	1,488

*Cumulative recovery per MMscf of original fluid in place.

**Primary separator at 800 psig and 80°F, reduced to 300 psig and 80°F for pressures below 1,200 psig; second stage at 50 psig and 80°F; stock tank at 0 psig and 80°F.

TABLE 10—HYDROCARBON ANALYSIS OF LEAN-GAS SAMPLE*

Component	Mol %	Gal/scf x 10 ³
Carbon dioxide	nil	
Nitrogen	nil	
Methane	94.68	
Ethane	5.27	1.401
Propane	0.05	0.014
Butanes plus	nil	nil
Total	100.00	1.415
Calculated gas gravity (air = 1.000)		0.580
Calculated gross heating value of dry gas at 14.65 psia at 60°F, Btu/ft ³		1,048

*Synthetically prepared in the laboratory.

TABLE 11—SOLUBILITY AND SWELLING TEST AT 200°F (Injection Gas/Lean Gas)

Mixture Number	Cumulative Gas Injected (scf/bbl)*	(mol fraction)**	Swollen Volume†	Dewpoint Pressure (psig)
0‡	0	0.0000	1.0000	3,428
1	190	0.1271	1.1224	3,635
2	572	0.3046	1.3542	4,015
3	1,523	0.5384	1.9248	4,610
4	2,467	0.6538	2.5043	4,880

*Cumulative cubic feet of injection gas at 14.65 psia and 60°F per barrel of original reservoir fluid at 3,428 psig and 200°F.

**Cumulative moles of injection gas per total moles of indicated mixture.

†Barrels of indicated mixture at its dewpoint pressure and 200°F per barrel of original reservoir fluid at 3,428 psig and 200°F.

‡Original reservoir fluid.

TABLE 12—PRESSURE/VOLUME RELATIONS OF MIXTURE 1 AT 200°F (Constant-Composition Expansion)

Pressure (psig)	Relative Volume*	Liquid Volume* (% saturated volume)
6,000	0.9115	—
5,502	0.9387	—
5,000	0.9719	—
4,500	1.0135	—
4,000	1.0687	—
3,800	1.0965	—
3,700	1.1116	—
3,650	1.1203	—
3,635	1.1224	0.0 (dewpoint)
3,600	1.1298	0.3
3,500	1.1508	1.7
3,300	1.1969	6.8
3,000	1.2918	12.8

*Relative volumes and liquid volume percents are based on the original hydrocarbon PV at 3,428 psig and 200°F.

TABLE 13—PRESSURE/VOLUME RELATIONS OF MIXTURE 2 AT 200°F (Constant-Composition Expansion)

Pressure (psig)	Relative Volume*	Liquid Volume* (% saturated volume)
6,000	1.1294	—
5,500	1.1686	—
5,000	1.2162	—
4,500	1.2767	—
4,300	1.3064	—
4,100	1.3385	—
4,050	1.3479	—
4,015	1.3542	0.0 (dewpoint)
3,950	1.3667	0.1
3,800	1.3992	0.5
3,400	1.5115	4.5
3,000	1.6709	9.4

*Relative volumes and liquid volume percents are based on the original hydrocarbon PV at 3,428 psig and 200°F.

TABLE 14—PRESSURE/VOLUME RELATIONS OF MIXTURE 3 AT 200°F (Constant-Composition Expansion)

Pressure (psig)	Relative Volume*	Liquid Volume* (% saturated volume)
6,000	1.6865	—
5,600	1.7413	—
5,300	1.7884	—
5,100	1.8233	—
5,000	1.8422	—
4,950	1.8519	—
4,900	1.8620	—
4,800	1.8827	—
4,700	1.9043	—
4,610	1.9248	0.0
4,500	1.9512	0.1
4,200	2.0360	0.3
3,900	2.1378	0.6
3,500	2.3193	2.1
3,000	2.6348	6.0

*Relative volumes and liquid volume percents are based on the original hydrocarbon PV at 3,428 psig and 200°F.

at and below the dewpoint pressure during cycling. Two companies (Elf Aquitaine and Petek) chose to match phase volumes in the swelling test only for pressures in the range expected to occur during cycling. We believe this to be a valid approach but do not know how this affects the cycling problem.

PVT Matches to the PVT Data

We asked for matches of total volume in constant-composition expansion, liquid dropout and equilibrium gas yield in constant-volume depletion, and swelling volume and dewpoint pressure during swelling of reservoir gas with lean gas. We also asked companies to describe techniques used for *K* values, phase densities and viscosities, and EOS parameters used for the PVT match.

The number of components used ranged from a low of 5 components (Chevron and Core Laboratories) to highs of 12 (Marathon) and 13 (Petek). A special model based on partial densities (McCord-Lewis) used 16 components to obtain the density data needed, but the reservoir cal-

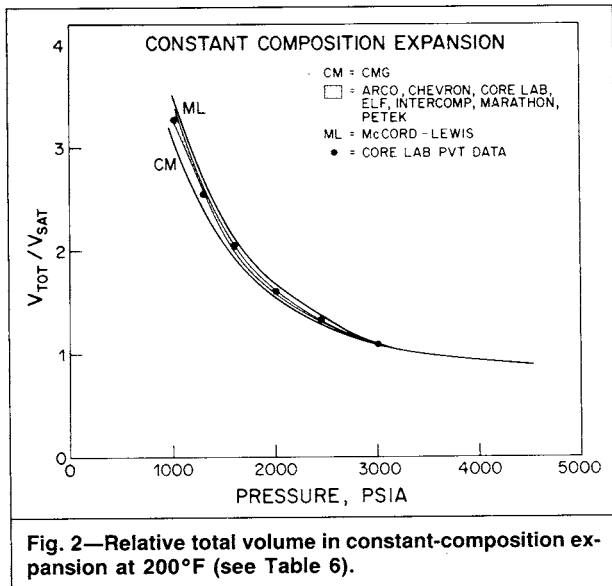


TABLE 15—PRESSURE/VOLUME RELATIONS OF MIXTURE 4 AT 200°F (Constant-Composition Expansion)

Pressure (psig)	Relative Volume*	Liquid Volume* (% saturated volume)
6,000	2.2435	—
5,500	2.3454	—
5,000	2.4704	—
4,880	2.5043	0.0 (dewpoint)
4,800	2.5288	Trace
4,600	2.5946	0.1
4,400	2.6709	0.3
4,000	2.8478	0.7
3,500	3.1570	1.4
3,000	3.5976	3.6

*Relative volumes and liquid volume percents are based on the original hydrocarbon PV at 3,428 psig and 200°F.

culations do not perform material balance on all 16 components. Table 16 indicates the component groups selected by each participant.

Tables 17 through 25 give summary data for each company's representation of component properties and the basic PVT match obtained with this set of components. More detailed matches of PVT data are included in Figs. 2 through 6.

Fig. 2 shows pressure/volume data in constant-composition expansion of the reservoir gas at 200°F [93°C]. While there are some minor discrepancies at the lowest pressures shown, there is rather good agreement in the pressure range in which most of the gas cycling takes place, between 2,500 and 3,400 psi [17.2 and 23.4 MPa].

Fig. 3 shows liquid dropout in constant-volume depletion. The greatest discrepancies occur in the neighbor-

hood of 2,500 psi [17.2 MPa] with peak liquid volume varying between about 18 and 22% of the initial (dew-point) gas volume. Actually, the reservoir models predict liquid volumes higher than this value in the vicinity of the production well because of convection of heavy end products into this low-pressure area and subsequent deposition. The increased heptanes-plus content leads to compositions and flash behavior not available in the laboratory data provided. Results given later show disagreement in the predicted liquid buildup in this area, which we attribute to the absence of flash data for such compositions.

Liquid yield by multistage surface separation of equilibrium gas produced during constant-volume depletion is given in Fig. 4. Separator conditions for the problem differ slightly from the separator conditions in the laboratory reports distributed to the participants in two areas: (1) the primary separator pressure is switched from 815

TABLE 16—COMPONENT GROUPINGS

Component	Arco	Chevron	Core Laboratories	CMG	Elf Aquitaine	Intercomp	Marathon	McCord-Lewis	Petek
CO ₂	X				X		X	X	X
N ₂	X							X	X
C ₁	X	X					X	X	X
C ₂	X	X					X	X	X
C ₃	X						X	XX	X
C ₄							X	XX	X
C ₅							X	X	X
C ₆							X	X	
C ₇							X	X	
C ₈							X	X	
C ₉							X	X	
C ₁₀								X	
C ₁₁								X	
H ₁	X	X	X	X	X	X	X	X	X
H ₂	X			X		X	X		X
H ₃	X					X			X
H ₄						X			X
H ₅						X			X
Total number of components	9	5	5	10	6	8	12	16	13
Total C ₆₊ components	—	2	—	—	2	—	6	7	—
Total C ₇₊ components	3	—	2	4	—	5	—	—	5

TABLE 17—CHARACTERIZATION DATA AND PVT MATCH, ARCO

Component Characterization Data						
Component	p_c (atm)	T_c (K)	Acentric Factor	Molecular Weight	Mole Fraction	
CO ₂	72.9	304.2	0.225	44.01	0.0121	
N ₂	33.5	126.2	0.040	28.01	0.0194	
C ₁	45.6	186.6	0.013	16.04	0.6599	
C ₂	48.2	305.4	0.098	30.07	0.0869	
C ₃	42.0	369.9	0.152	44.10	0.0591	
C ₄₋₆	33.9	396.2	0.234	67.28	0.0967	
C _{7P₁}	25.6	572.5	0.332	110.9	0.0472	
C _{7P₂}	16.7	630.2	0.495	170.9	0.0153	
C _{7P₃}	8.50	862.6	0.833	282.1	0.0034	

Interaction Coefficients						
CO ₂	0					
N ₂	-0.02	0				
C ₁	0.10	0.036	0			
C ₂	0.13	0.05	0	0		
C ₃	0.135	0.08	0	0	0	
C ₄₋₆	0.1277	0.1002	0.09281	0	0	0
C _{7P₁}	0.1	0.1	0	0.00385	0.00385	0 0
C _{7P₂}	0.1	0.1	0	0.00630	0.00630	0 0 0
C _{7P₃}	0.1	0.1	0.1392	0.00600	0.00600	0 0 0 0

PVT Methods
Peng-Robinson EOS³ for vapor/liquid equilibrium and densities. Viscosity for gas and liquid by Lohrenz *et al.*⁴

Initialization Results

Initial wet gas in place, Bscf	26.58
Initial separator gas in place, Bscf	24.06
Initial stock-tank oil in place, MMSTB	3.373

Basic PVT Match

Dewpoint pressure, psia	3480
Dewpoint Z factor	0.811

Simulator Description
Standard IMPES compositional reservoir simulator with Gauss D4⁵ linear equation solution technique.

TABLE 18—CHARACTERIZATION DATA AND PVT MATCH, CHEVRON

Component Characterization Data					
Component	p_c (atm)	T_c (K)	Acentric Factor	Molecular Weight	Mole Fraction
C ₁	45.8	190.7	0.0130	16.04	—
C ₂	48.2	305.4	0.0986	30.07	—
C ₃₋₅	37.4	409.2	0.1825	54.85	—
C ₆₋₁₀	28.8	568.2	0.3080	103.5	—
C ₁₁₊	18.1		0.5449	191.0	—

Interaction Coefficients					
C ₁	0				
C ₂	0	0			
C ₃₋₅	-0.0997	-0.1241	0		
C ₆₋₁₀	-0.0044	-0.2765	0.010	0	
C ₁₁₊	0.1355	0.2492	0.010	0	0

PVT Methods
Peng-Robinson EOS³ for vapor/liquid equilibrium and densities. Viscosity for gas and liquid by Lohrenz *et al.*⁴

Initialization Results

Initial wet gas in place, Bscf	28.5
Initial separator gas in place, Bscf	25.3
Initial stock-tank oil in place, MMSTB	3.66

Basic PVT Match

Dewpoint pressure, psia	3501
Dewpoint Z factor	0.7538

Simulator Description
Chevron's finite-difference simulator was used for all reservoir calculations. Gauss with D4 ordering⁵ for pressure solution was used.

to 315 psia [5.6 to 2.2 MPa] at average reservoir pressure of 2,500 psia [17.2 MPa] in the reservoir model, whereas the laboratory assumed a separator pressure switch at a pressure of 1,200 psig [8.3 MPa], and (2) the stock-tank separator temperature is taken as 60°F [16°C] for the reservoir model, whereas the laboratory data were based on an 80°F [27°C] stock-tank temperature.

Participants were asked to match surface yield for the laboratory separator conditions. Core Laboratories provided computations for multistage separator products with experimentally determined equilibrium gas compositions in Table 8 for the separator conditions specified in the model problem. These data were not distributed to the participants but are shown in Fig. 4.

As seen in Fig. 4, the greatest difference in yield by these two sets of separator conditions is at the dewpoint pressure and is a result of the colder stock-tank temperature used in the reservoir model. Participants whose data differed significantly from the average were offered opportunities to review their results in light of the trends, and in two cases rematches were obtained. The reservoir model is significantly affected by the match of Fig. 4. These data are influenced by K values during depletion, surface liquid density correlations, and surface separator K values.

The relative volumes of reservoir gas blends with increasing amounts of lean gas and the dewpoint pressures of these various blends are shown in Figs. 5 and 6. Several participants expressed skepticism regarding the need to match this part of the PVT data for reservoir modeling purposes, and this should be kept in mind when these figures are evaluated. Two concerns were expressed.

1. The actual injection gas derived from the models has a molecular weight of about 22, whereas the lean-gas

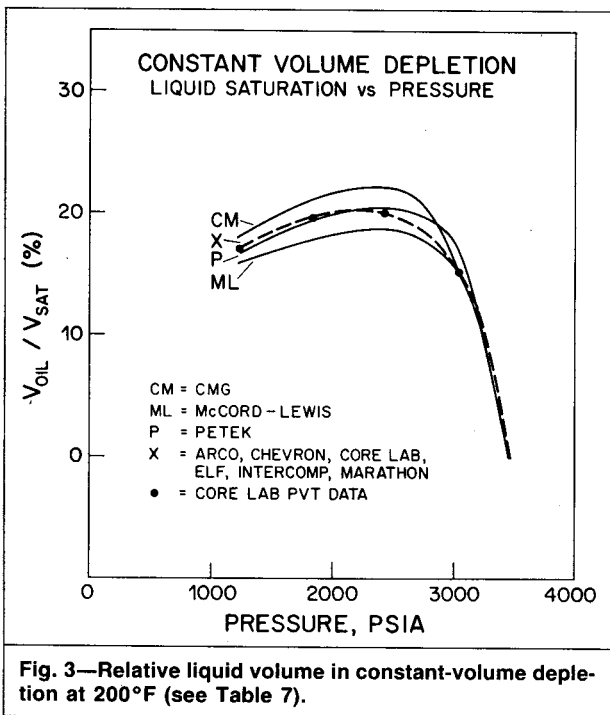


Fig. 3—Relative liquid volume in constant-volume depletion at 200°F (see Table 7).

TABLE 19—CHARACTERIZATION DATA AND PVT MATCH, CORE LABORATORIES

Component Characterization Data					
Component	p_c (psi)	T_c (°R)	T_b (°R)	Molecular Weight	Density (g/cm ³)
C ₇	397	973	688	94	0.711
C ₈	361	1,024	756	110	0.739
C ₉	332	1,070	822	117	0.766
C ₁₀	304	1,112	886	137	0.777
C ₁₁₊	232	1,250	*	213.6	0.814
C ₇₊	—	—	—	140	0.773

Interaction Coefficients
Not available

PVT Methods
A 16-component PVT simulator was used to prepare *K*-value data by convergence pressure techniques. Slight heavy-component *K*-value adjustment was used to match dewpoint pressure, liquid volumes, and depletion-gas compositions. Once a satisfactory match was obtained, results from the 16-component PVT simulator were used as the basis for tables of input data to the compositional model. The compositional model used five pseudocomponents, with properties of the model components representing groups of components between CO₂ and C₁₀ computed as functions of pressure during the laboratory data match. Stiel-Thodos viscosity correlations were used for oil and gas. Gas *Z* factor was obtained with Yarborough-Hall fit of Standing-Katz charts. Liquid density was obtained with modified Standing correlations. *K* values were fit with methods suitable for the kind of pseudocomponent (lights, heavies, and nonhydrocarbons). Note offered by Core Laboratories: The injection gas of bulked separators contains 22% CO₂ and heavier, a gas considerably heavier than the injection gas used in the laboratory PVT studies. Therefore, the laboratory data on the various lean-gas/reservoir-fluid mixtures are of little use in developing the properties of mixtures of bulked separator gas and reservoir fluid. (They do, however, provide a comparison of calculated and measured gas deviation factors.) Core Laboratories thus used the Peng-Robinson EOS³ to estimate dewpoints of mixtures of reservoir fluid with separator gas expected in the model. *K* values obtained were fitted with convergence pressure as the parameter for composition dependence for mixtures of this nature.

Initialization Results

Initial wet gas in place, Bscf	26.37
Initial separator gas in place, Bscf	23.04
Initial stock-tank oil in place, MMSTB	3.689

Basic PVT Match

Dewpoint pressure, psia	3443
Dewpoint <i>Z</i> factor	0.803

Simulator Description
Core Laboratories' compositional model uses up to six components. Five components were used for the present problem, with *K* values prepared as discussed above. Core Laboratories has a version of its PVT simulator that uses the Peng-Robinson EOS³ but it was not used in this problem.

TABLE 20—CHARACTERIZATION DATA AND PVT MATCH, CMG

Component Characterization Data					
Component	p_c (atm)	T_c (K)	Acentric Factor	Molecular Weight	Mole Fraction
C ₇₋₉	26.25	573.45	0.3613	114.4	0.0399
C ₁₀₋₁₁	23.18	637.79	0.4501	144.8	0.0122
C ₁₂₋₁₄	19.99	685.75	0.5339	177.8	0.0080
C ₁₅₊	12.55	748.33	0.7244	253.6	0.0058

Interaction Coefficients
Not available

PVT Methods
Peng-Robinson EOS³ for vapor/liquid equilibrium and densities. Viscosities for gas and liquid by Jossi-Stiel-Thodos.⁶

Initialization Results

Initial wet gas in place, Bscf	26.37
Initial separator gas in place, Bscf	22.90
Initial stock-tank oil in place, MMSTB	3.39

Basic PVT Match

Dewpoint pressure, psia	3443
Dewpoint <i>Z</i> factor	0.8030

Simulator Description
CMG's IMPES simulator, MISIM3,⁷ uses a quasi-Newtonian method of solution called QNSS⁸ developed at CMG. Preconditioned conjugate gradients are used to solve the diagonally dominant matrix equations. QNSS was also used to solve the flash obtained from the Peng-Robinson EOS.³ Pseudocomponent selection is based on unpublished methods developed at CMG.

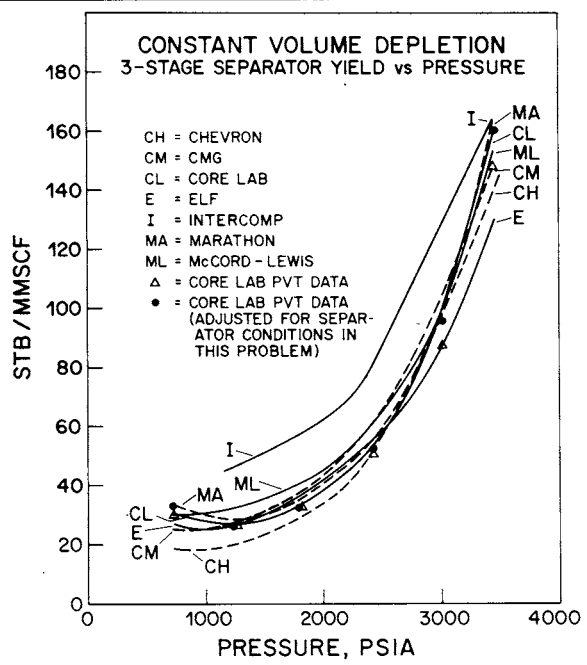


Fig. 4—Three-stage separator yield in constant-volume depletion at 200°F (see Table 9).

TABLE 21—CHARACTERIZATION DATA AND PVT MATCH, ELF AQUITAINE

Component Characterization Data					
Component	p_c (psi)	T_c (°R)	Acentric Factor	Molecular Weight	V_c (ft ³ /lbm)
CO ₂	1,069.52	547.56	0.2250	44.01	0.034
C ₁ + N ₂	667.00	343.08	0.0115	16.04	0.099
C ₂	708.18	549.72	0.0908	30.07	0.079
C ₃ - C ₅	545.93	729.27	0.1763	54.84	0.071
C ₆ - C ₁₀	363.66	959.67	0.3760	108.75	0.068
C ₁₁₊	223.30	1,139.67	0.7790	211.78	0.066

Interaction Coefficients
Not available

PVT Methods
Elf Aquitaine's EQLV PVT package based on the Peng-Robinson EOS³ was used for the PVT match. Viscosity correlation used was Lohrenz *et al.*⁴ Note offered by Elf Aquitaine: Results of the saturation pressure match are poor, but the constant composition expansion data (of total volume and liquid drop out) agreed fairly well with the calculations for each mixture. From Elf Aquitaine's experience, a very detailed composition analysis (up to C₃₀₊) would be necessary to match such results adequately, with a very small slope of liquid deposit curve at dewpoint. Hence the match was based on the liquid deposit at 3,000 psig.

Initialization Results

Initial wet gas in place, Bscf	26.50
Initial separator gas in place, Bscf	23.05
Initial stock-tank oil in place, MMSTB	3.42

Basic PVT Match

Dewpoint pressure, psia	3,443
Dewpoint Z factor	0.8027

Simulator Description
Elf Aquitaine's MULTIKIT compositional model was used. It allows for either *K*-value tables (algebraic) convergence pressure relations, or EOS (Peng-Robinson) *K* values. In this study, *K*-value tables based on component C₁ global mole fraction were used based on precalculations with the Peng-Robinson EOS.³ Phase densities were also obtained from the EOS. Kazemi *et al.*'s⁹ formulation of the IMPES equation is used. Matrix solution is by Gauss elimination on D4 ordering. Both five- and nine-point differences were used, but results based on the nine-point solution are shown. Differences between the two methods were small in this problem.

TABLE 22—CHARACTERIZATION DATA AND PVT MATCH, INTERCOMP

Component Characterization Data					
Component	Acentric Factor a	Acentric Factor b	Specific Gravity	Molecular Weight	Mole Fraction
F ₇	0.37348	0.08141	0.7383	108.35	0.03672
F ₈	0.45723	0.07779	0.7787	151.90	0.01764
F ₉	0.45723	0.07779	0.8112	196.68	0.00721
F ₁₀	0.52310	0.08525	0.8452	254.22	0.00370
F ₁₁	0.45624	0.06329	0.8907	353.24	0.00062

Interaction Coefficients
Not available

PVT Methods
Intercomp's PVT package is equipped with four choices of EOS's. The Peng-Robinson EOS³ was used for this problem. Regression methods are used for the PVT data match.¹⁰ Pseudocomponents were developed by a special version of Whitson's split-out procedure,¹¹ followed by component lumping to a total of eight components. Viscosity was based on Lohrenz *et al.*,⁴ and all phase and equilibrium data were derived from the EOS. Note offered by Intercomp: The Peng-Robinson EOS used for the comparative solution project was only calibrated vs. measured data from tests performed at reservoir conditions. No adjustments of the EOS parameters were made to represent the fluid behavior at surface conditions. The reasons for omitting the EOS match of surface conditions can be summarized as follows. The separator compositions and recombination ratio presented in the PVT report are considered not to be representative of a vapor/liquid equilibrium state at 72°F and 2,000 psig. Even if the data do represent equilibrium, the pressure at recombination is considered too far removed from the separator pressures used in the performance simulation to render meaningful calibration of the EOS for surface conditions. The cumulative surface recoveries from the constant-volume expansion presented in the PVT report were calculated with published equilibrium ratios. No attempts were made to match these data because that would involve calibrating the EOS vs. a correlation. In the absence of measured surface yields, no conclusions can be drawn regarding the validity of the EOS or the *K*-value correlation.

Initialization Results

Initial wet gas in place, Bscf	26.53
Initial separator gas in place, Bscf	23.29
Initial stock-tank oil in place, MMSTB	3.76

Basic PVT Match

Dewpoint pressure, psia	3,443
Dewpoint Z factor	0.7917

Simulator Description
Intercomp's COMP-II was used for the reservoir model.¹² It is a modified IMPES simulator with generalized cubic EOS calculations for phase equilibrium and phase density calculations. A special technique, the stabilized IMPES method,¹³ is used to overcome timestep size limitations inherent in IMPES models.

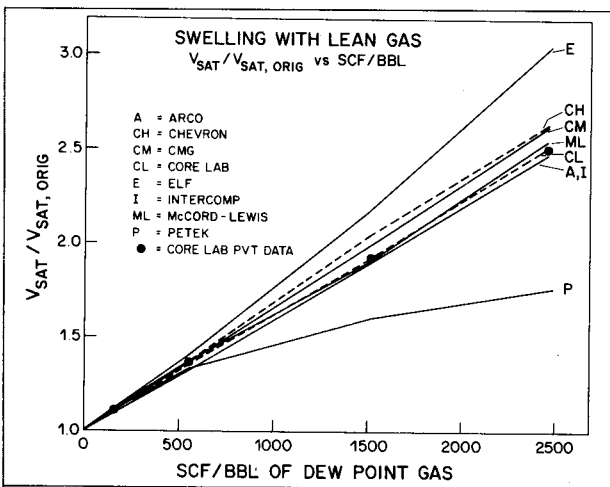


Fig. 5—Relative total volume in swelling of reservoir gas with lean hydrocarbon gas at 200°F (see Table 11).

molecular weight is about 17. Differences in the swelling characteristics obtained with these gases would be expected.

2. The reservoir pressure falls continuously with time in both cases of interest. Thus volumetric behavior at pressures above the initial reservoir pressure is unimportant in the context of the model.

Reservoir Model Performance

Table 26 gives the initial surface fluids in place with multistage separation. Stock-tank oil rates for constant gas sales rate and for deferred early gas sales are shown in Figs. 7 and 8. The corresponding cumulative liquid pro-

TABLE 23—CHARACTERIZATION DATA AND PVT MATCH, MARATHON

Component Characterization Data					
Component	p_c (atm)	T_c (K)	Acentric Factor	Molecular Weight	Mole Fraction
C ₆	34.53	504.3	0.2592	81.00	0.0181
C ₇	33.50	520.6	0.2778	88.00	0.0144
C ₈	31.81	533.3	0.2977	95.00	0.0150
C ₉	30.07	550.4	0.3240	104.00	0.0105
Gas	25.97	598.2	0.4035	130.00	0.0122
Oil	20.00	693.0	0.6000	275.00	0.0138

Interaction Coefficients
Not available

PVT Methods

Marathon used the Peng-Robinson³ EOS as a starting point for *K*-value tables. Hand methods and adjustments of *K* values generally allow a more precise description of equilibrium data in the two-phase region than by unmodified *K* values. Phase densities are also obtained by adjustments to EOS values in such a manner as to allow a match to observed volumetric data and to reported *Z* factors in depletion experiments. Oil viscosity was obtained from the correlation of Little and Kennedy¹⁴ and gas viscosity by the Lee¹⁵ correlation.

Initialization Results

Initial wet gas in place, Bscf	26.39
Initial separator gas in place, Bscf	22.98
Initial stock-tank oil in place, MMSTB	3.73

Basic PVT Match

Dewpoint pressure, psia	3,443
Dewpoint <i>Z</i> factor	0.8035

Simulator Description

Marathon's IMPES simulator is based on the Kazemi *et al.*⁹ pressure equation and all PVT data are entered as tables. In the present problem, *K* values were functions of pressure only, but phase densities and viscosities were adjusted to match both depletion data and estimated bulk-separator gas properties.

duction for these cases is given in Figs. 9 and 10. All yearly production data were connected with straight-line segments in Figs. 7 through 10. Most models were already below the dewpoint pressure at 1 year of production, and surface liquid rate had already dropped below initial rate. For most participants, primary separator switchout occurred late in the cycling phase (10 years).

In most cases, the predicted surface oil rate is closely correlated with the liquid yield predictions shown in Fig. 4. However, this is not the sole explanation for the discrepancies in early oil rate seen in both cycling cases. We believe the predicted pressure in early years of cycling is also important.

Swelling data matches in Fig. 5 can be used to find molar volumes of reservoir gas saturated with additions of lean gas. For the reservoir model, more pertinent data are molar volumes (*Z* factors) of mixtures at typical cycling pressures, because this determines average reservoir pressure for a given excess of production over injection. Some limited mixture volume data were available from the laboratory reports at 3,000 psi [20.7 MPa] and above (Tables 12 through 15), but matches to these data were not requested.

During the critical early years, the pressure decline is affected by *Z* factors for reservoir gas, injection gas, and gas mixtures, as well as by the rates of wet-gas produced and separator-gas recycled. The rate of gas recycled for

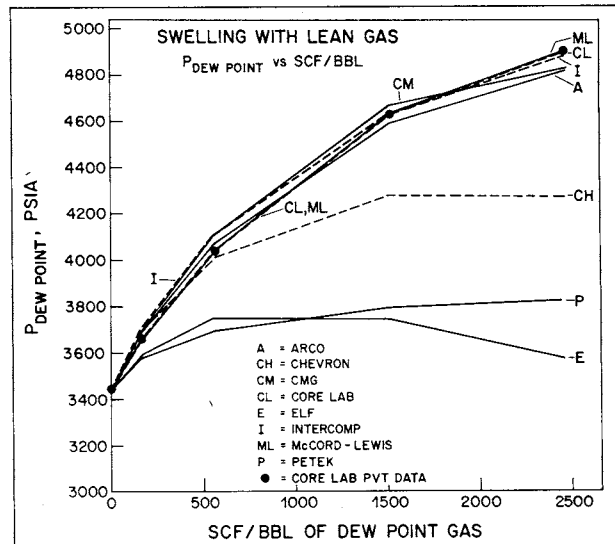


Fig. 6—Dewpoint pressure during swelling of reservoir gas with lean hydrocarbon gas at 200°F (see Table 11).

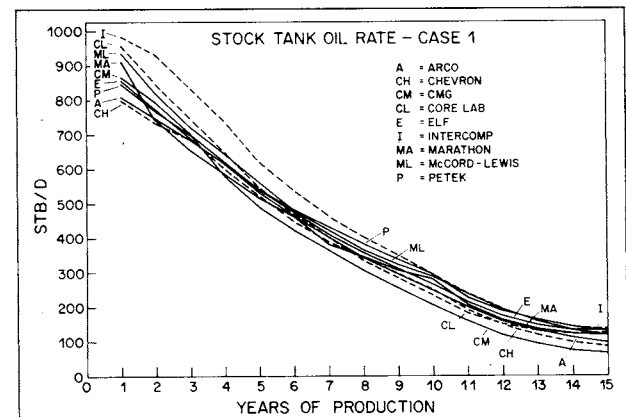


Fig. 7—Reservoir model stock-tank oil rate, Case 1.

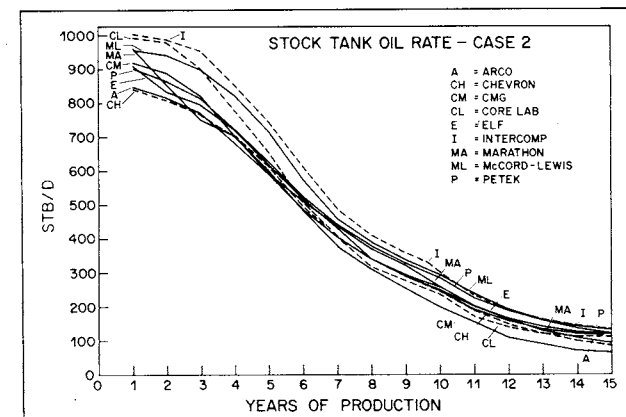


Fig. 8—Reservoir model stock-tank oil rate, Case 2.

TABLE 24—CHARACTERIZATION DATA AND PVT MATCH, McCORD-LEWIS

Component Characterization Data						
Component	p_c (psi)	T_c (°F)	Acentric Factor	Molecular Weight	Specific Gravity	T_b (°F)
C ₁	673.1	343.3	0.0130	16.04	0.3250	201.0
C ₂	708.3	549.8	0.0986	30.07	0.4800	332.2
C ₃	617.4	665.8	0.1524	44.09	0.5077	416.0
iC ₄	529.1	734.6	0.1848	58.12	0.5631	470.6
nC ₄	550.7	765.4	0.2010	58.12	0.5844	490.8
iC ₅	483.5	828.7	0.2223	72.15	0.6248	541.8
nC ₅	489.5	845.6	0.2539	72.15	0.6312	556.6
C ₆	457.1	910.1	0.2806	84.00	0.6781	607.0
C ₇	432.2	969.6	0.3220	101.20	0.7100	657.0
C ₈	419.7	1,011.7	0.3495	114.60	0.7340	692.0
C ₉	391.6	1,064.8	0.3912	128.80	0.7570	740.0
C ₁₀	365.0	1,118.9	0.4354	142.30	0.7800	790.0
C ₁₁	359.2	1,154.7	0.4568	155.00	0.8010	820.0
C ₁₂₊	348.0	1,219.7	0.4946	210.00	0.8380	875.0
CO ₂	1,071.3	547.6	0.2250	44.01	0.4200	350.7
N ₂	492.3	227.2	0.0400	28.02	0.4800	139.6

Interaction Coefficients (with methane)

C ₆	C ₇	C ₈	C ₉	C ₁₀	C ₁₁	C ₁₂₊	CO ₂	N ₂
0.02813	0.03260	0.03596	0.03918	0.04240	0.04534	0.12860	0.10000	0.1000

PVT Methods

McCord-Lewis used Watson¹⁶ characterization factors for each fraction with correlations of Whitson and Haaland.^{11,17,18} Boiling points, with some minor changes, came from Katz and Firoozabadi.¹⁹ Specific gravities and methane binary interaction coefficients of the heavy ends were estimated from the Watson K factor. Lee-Kesler^{20,21} correlations were used for critical pressure and temperature and molecular weight.

Initialization Results

Initial wet gas in place, Bscf	26.52
Initial separator gas in place, Bscf	23.18
Initial stock-tank oil in place, MMSTB	3.56

Basic PVT Match

Dewpoint pressure, psia	3,443
Dewpoint Z factor	0.803

Simulator Description

The McCord-Lewis simulator is based on a partial density model that includes condensation from the reservoir gas phase to the reservoir liquid phase. The basic assumption is that each reservoir phase can be viewed as a binary mixture of its surface products, termed partial densities, when forming any reservoir phase. The detailed discussion of the model is not possible here, but it is important to note that it doesn't require K values per se.

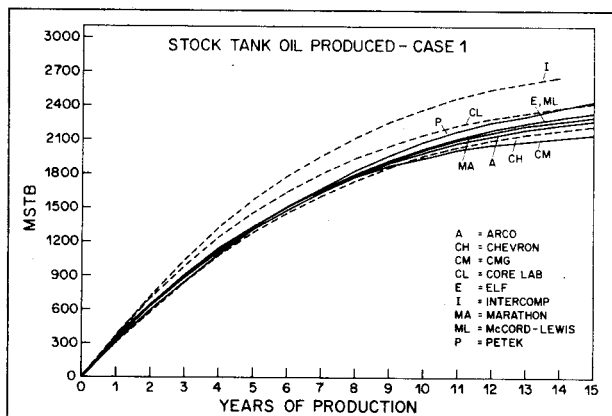


Fig. 9—Cumulative reservoir model stock-tank oil produced, Case 1.

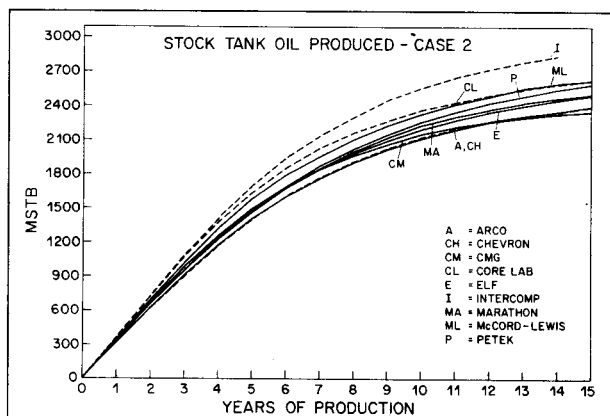


Fig. 10—Cumulative reservoir model stock-tank oil produced, Case 2.

TABLE 25—CHARACTERIZATION DATA AND PVT MATCH, PETEK

Component Characterization Data						
Component	p_c (MPa)	T_c (K)	Acentric Factor	Molecular Weight	V_c (cm ³ /mol)	Mole Fraction
HC ₁₀	3.000	510.0	0.3498	100.2	420.0	0.0144
HC ₂₀	3.000	560.0	0.3846	120.7	510.0	0.0326
HC ₃₀	2.500	630.0	0.5015	157.7	660.0	0.0083
HC ₄₀	2.100	700.0	0.8000	247.6	1,000.0	0.0104
HC ₅₀	1.200	960.0	0.9000	500.0	1,050.0	0.0002

Parameter Matching Process (Weight Factors on Acentric Factors)		
Component	Acentric Factor a	Acentric Factor b
HC ₁₀	1.160840	1.00000
HC ₂₀	0.993215	1.00000
HC ₃₀	0.791887	1.00000
HC ₄₀	1.032080	1.00092
HC ₅₀	1.032080	1.00092

Interaction Coefficients
Not available

PVT Methods
Petek used the Peng-Robinson EOS³ for K value and density data. Viscosities were calculated from the Lohrenz *et al.*⁴ model. Petek made no attempt to match the solubility data of lean-gas injections with reservoir gas as it lacked importance in the context of the model. Instead, liquid relative volumes from the constant-composition expansions of the various mixtures were carefully matched in the range of reservoir pressures. This was felt to have a larger effect on correct prediction of reservoir performance.

Initialization Results

Initial wet gas in place, Bscf	28.28
Initial separator gas in place, Bscf	24.70
Initial stock-tank oil in place, MMSTB	3.57

Basic PVT Match

Dewpoint pressure, psia	3,452
Dewpoint Z factor	0.7532

Simulator Description
The Petek simulator is IMPES and uses one of several cubic EOS choices for PVT calculations. The first version of a joint project venture has recently been released. SIP²² was used in the current problem to solve the pressure equations. Automatic timestep selection was used and found to be helpful in the problem.

TABLE 26—INITIAL FLUIDS IN PLACE

Company	Wet Gas (Bscf)	Dry Gas (Bscf)	Stock-Tank Oil (MMSTB)
Arco	26.58	24.06	3.373
Chevron	28.5	25.3	3.66
Core Laboratories	26.37	23.04	3.689
CMG	26.37	22.90	3.39
Elf Aquitaine	26.50	23.05	3.42
Intercomp	26.53	23.29	3.76
Marathon	26.39	22.98	3.73
McCord-Lewis	26.52	23.18	3.56
Petek	28.28	24.7	3.57

each cycling case is fixed in this problem. The wet gas produced depends on the surface separator efficiency because the separator-gas rate is specified. The wet-gas rate thus depends on the match to yield data in Fig. 4 and surface-liquid molar density. We did not request predicted surface-liquid molar density from the PVT matches. The initial molar rate of separator-gas recycled is approximately 0.67 times the rate of wet-gas production in Case 1, allowing for sales gas. The ratio is 0.76 as the liquid content of the produced-gas approaches zero.

At dewpoint pressure, the injection-gas Z factor is approximately 6% higher than the reservoir-gas Z factor, and Z factors of mixtures of these gases should be some-

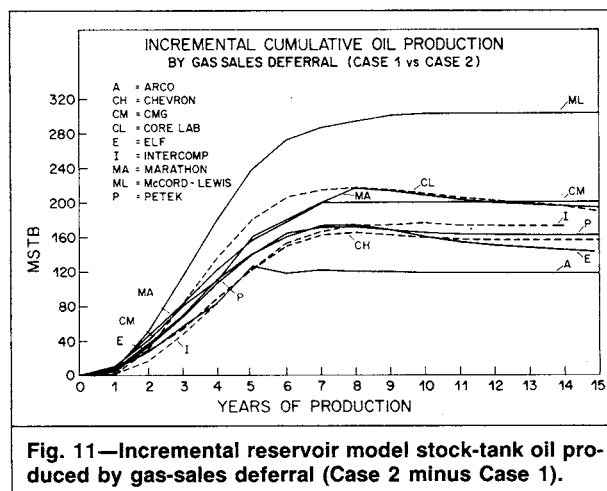


Fig. 11—Incremental reservoir model stock-tank oil produced by gas-sales deferral (Case 2 minus Case 1).

TABLE 27—AVERAGE OIL SATURATION, CASE 1 (%)

Company	Year	Layer 1	Layer 2	Layer 3	Layer 4
Arco	1	3.06	3.20	3.12	2.78
	5	3.57	7.80	10.22	7.32
	10	2.12	6.51	10.78	5.61
	15	1.87	5.36	8.55	4.71
Chevron	1	1.76	1.89	1.78	1.57
	5	3.32	6.82	8.96	6.94
	10	2.10	6.87	11.89	6.79
	15	2.18	6.78	11.01	6.58
Core Laboratories	1	1.1	1.1	0.8	0.5
	5	3.1	7.6	9.6	7.0
	10	1.9	7.0	10.8	5.9
	15	1.5	5.6	8.5	4.6
CMG	1	2.27	2.48	2.37	2.03
	5	2.73	7.95	11.08	8.37
	10	1.26	5.56	11.27	6.43
	15	1.10	4.55	8.44	5.23
Elf Aquitaine	1	3.34	3.60	3.59	3.06
	5	3.24	7.82	10.30	7.72
	10	1.56	6.55	10.84	5.83
	15	1.31	5.28	8.65	4.74
Intercomp	1	0.78	0.81	0.75	0.62
	5	2.74	6.58	8.97	6.57
	10	1.52	5.55	9.89	5.42
	15	—	—	—	—
Marathon	1	4.28	4.60	4.60	4.04
	5	4.76	10.70	13.10	10.40
	10	2.55	8.16	11.94	7.01
	15	1.91	6.24	9.22	5.25
McCord-Lewis	1	1.10	1.07	1.01	0.81
	5	4.68	9.10	11.90	8.72
	10	2.87	6.30	11.42	5.98
	15	2.80	5.72	9.90	5.28
Petek	1	3.34	3.55	3.40	2.87
	5	3.58	8.26	11.15	8.72
	10	1.73	6.18	11.01	6.29
	15	1.45	5.04	8.75	5.24

TABLE 28—AVERAGE OIL SATURATION, CASE 2 (%)

Company	Year	Layer 1	Layer 2	Layer 3	Layer 4
Arco	1	0.97	0.86	0.73	0.51
	5	1.40	3.62	5.30	3.36
	10	1.31	5.18	9.93	4.94
	15	1.20	4.43	7.98	4.20
Chevron	1	0.55	0.46	0.39	0.34
	5	1.04	2.55	3.63	2.71
	10	1.26	5.37	10.99	6.01
	15	1.33	5.52	10.28	5.77
Core Laboratories	1	0	0	0	0
	5	0.9	3.1	5.0	2.9
	10	0.9	5.2	10.0	4.9
	15	0.8	4.2	7.8	3.9
CMG	1	0.0	0.0	0.0	0.0
	5	0.69	2.44	4.20	2.95
	10	0.51	3.56	9.70	5.71
	15	0.45	3.13	7.44	4.60
Elf Aquitaine	1	0.76	0.76	0.63	0.36
	5	1.23	3.91	6.70	4.20
	10	0.75	4.66	9.89	5.02
	15	0.66	3.92	7.95	4.24
Intercomp	1	0.10	0.08	0.03	0.01
	5	0.66	1.83	3.03	1.94
	10	0.76	3.77	8.76	4.55
	15	—	—	—	—
Marathon	1	1.89	1.98	1.94	1.57
	5	2.40	6.08	9.43	6.82
	10	1.71	6.40	11.45	5.73
	15	1.35	4.94	8.79	4.35
McCord-Lewis	1	0.0	0.0	0.0	0.0
	5	1.33	3.05	5.15	3.48
	10	1.10	3.43	9.30	4.62
	15	1.00	3.38	8.40	4.20
Petek	1	0.08	0.01	0.02	0.0
	5	1.16	3.32	5.76	4.07
	10	0.89	4.39	9.91	5.54
	15	0.76	3.76	8.01	4.61

where between the two. Discrepancies in pressure are affected by both wet-gas rate (determined by yield, Fig. 4, and surface-liquid density) and assumed gas Z factors in early years of cycling.

A partial compensation for this sensitivity to injection and production-gas Z factors is numerical dispersion, which tends to smear out the initial molecular weight and Z-factor contrast between injection and production gases. This and the merging of the participants' depletion matches (Fig. 4) at pressures far below dewpoint pressure explain the near-parallel oil production rates in the advanced stages of cycling and blowdown. Another factor compensating for discrepancies in Z factors and separator factors is the reservoir response to falling pressure. Any model with a high rate of decline in pressure produces a rapid loss in surface liquid yield. This reduces reservoir voidage and tends to lessen subsequent pressure decline.

Actual recovery efficiencies achieved by the models are atypical of field values in view of the homogeneous nature of the model grid. The results for liquid recovery are 55 to 74% of the initial oil (condensate) in place. The incremental production achieved by gas-sales deferral is shown in Fig. 11. These exhibit a considerable range—from 3 to 8% of the initial condensate in place.

Layer average oil saturations for selected times are given in Tables 27 and 28. Not surprisingly, these show

common trends of relatively uniform saturations for the first year. For other times, Layer 3 (the tight layer) shows high saturation because little injected gas sweeps this layer. Conversely, Layer 1 (a high-permeability layer) shows almost no liquid. Layers 2 and 4 are intermediate in sweep efficiency.

Condensate saturation in Node (7,7,4) is shown in Figs. 12 and 13. Most of the models achieve a fairly stable saturation of slightly more than irreducible oil saturation (24%). This indicates a condition of reservoir condensate flow in this area. Before this time, liquid dropout in the low-pressure region strips liquid from the gas stream. This continues until a small liquid flow begins and the surface yield stabilizes. The stabilized yield value depends on the mixing of injection gas with reservoir gas around the producer and the contribution of the depleted area behind the producer to production.

Later, during cycling, the condensate around the producer is partly revaporized, and reservoir oil ceases to flow. Liquid yield is partly sustained as some heavy-end fractions continue to vaporize and are produced. What is perhaps surprising is the widely different predictions for oil saturation at advanced depletion levels in the models, ranging from 0 to more than 22%. We believe that this can be explained by the K values used.

We made two supplementary runs with COMPIII²³ for Case 2 to demonstrate the importance of the K-value tech-

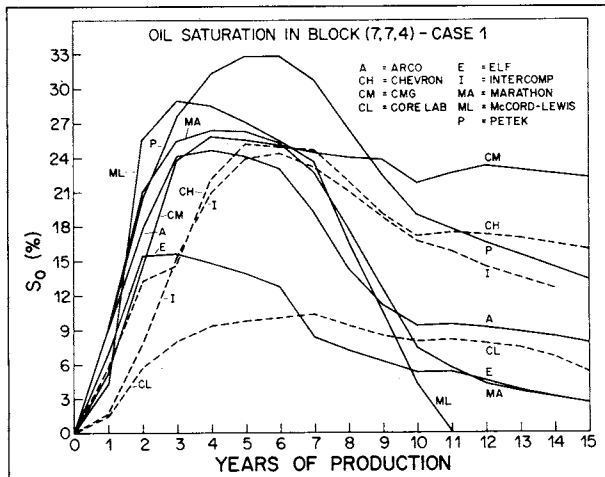


Fig. 12—Reservoir model condensate saturation in Block (7,7,4), Case 1.

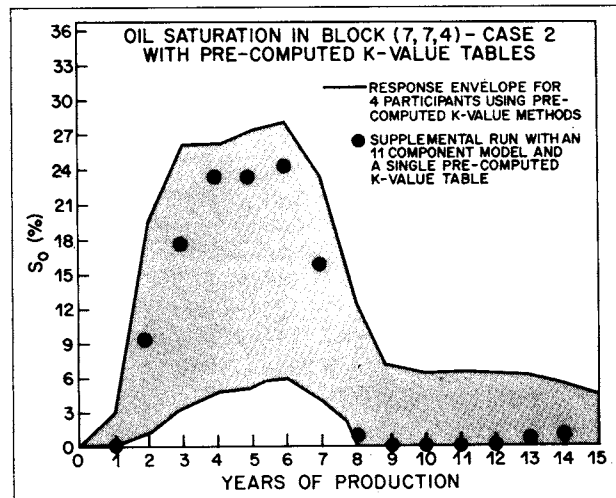


Fig. 14—Reservoir model condensate saturation in Block (7,7,4) with precomputed K-value tables, Case 2.

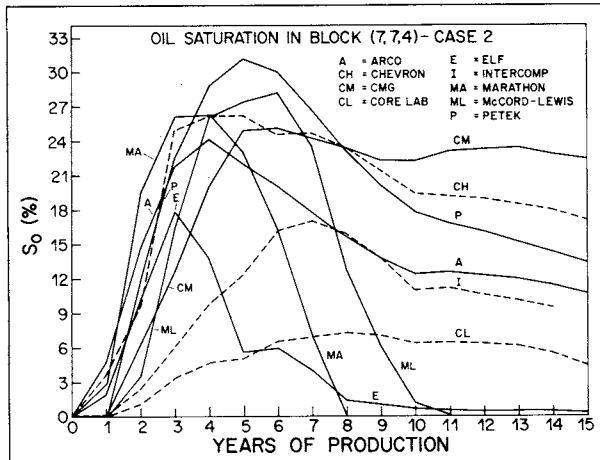


Fig. 13—Reservoir model condensate saturation in Block (7,7,4), Case 2.

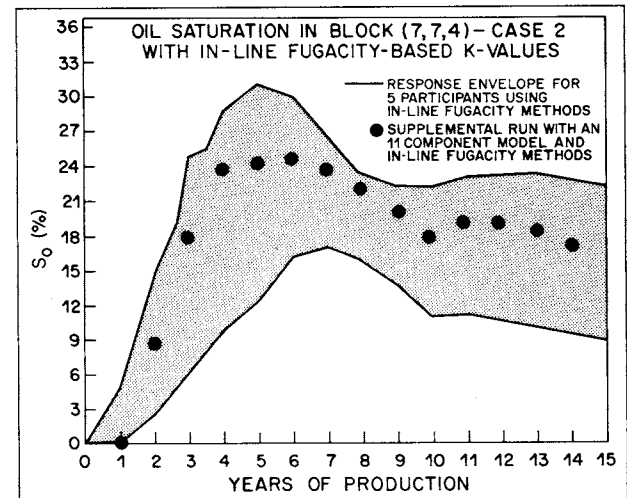


Fig. 15—Reservoir model condensate saturation in Block (7,7,4) with in-line fugacity-based K values, Case 2.

TABLE 29—RESERVOIR MODEL PERFORMANCE

Company	Numerical Solution Method	Computer Used	Number of Timesteps		Average Timestep Size (days)		Average CPU per Timestep		Material Balance Error at 15 years	
			1	2	1	2	1	2	1	2
Arco	IMPES	IBM 4341	325	—	16.8	—	121	—	2.0×10^{-3}	—
Chevron	IMPES	VAX-11/780	375	383	14.6	14.3	116	103	4.6×10^{-3}	8.0×10^{-4}
Core Laboratories	IMPES	CDC 6600	251	244	21.7	22.3	6.7	6.3	7.5×10^{-4}	6.6×10^{-4}
CMG	IMPES	Honeywell DPS 68	200	194	27.4	28.2	185.7	163	6.0×10^{-5}	3.1×10^{-5}
Elf Aquitaine	IMPES	IBM 3081	185	199	29.4	27.4	2.2	—	1×10^{-4}	—
Intercomp	IMPES	Harris 800	128	114	39.9	44.8	66.4	67.1	5.6×10^{-6}	—
Marathon	IMPES	Burroughs B7900	365	347	14.7	15.4	8.0	7.5	5.5×10^{-4}	5.7×10^{-4}
McCord-Lewis	IMPES	VAX-11/780	91	91	60.0	60.0	13.9	13.9	7.5×10^{-4}	—
Petek	IMPES	ND-560	519	509	10.5	10.7	168	192	1.1×10^{-3}	2.0×10^{-3}

nique. This compositional simulator permits K values to be entered as a table or as calculated in line in the normal manner with an EOS. For the run with K values as tables, we used a single K -value table with a constant-volume depletion of the reservoir gas and assumed K values were independent of composition. The supplementary runs made were identical in all respects except for the treatment of K values.

Figs. 14 and 15 show condensate saturation for the supplemental runs. Fig. 14 shows a clear indication of high evaporation rate of condensate obtained with a K -value table. Fig. 14 includes the response envelope of companies (Core Laboratories, Elf Aquitaine, Marathon, and McCord-Lewis) that used precomputed K -value tables. It shows a considerable scatter in predicted condensate, but all show rapid condensate evaporation in the late stages of cycling.

Fig. 15 shows condensate saturation for the supplemental run with 11 components and in-line K values with an EOS. The response envelope for all companies who used similar in-line K values is also shown. These show somewhat better agreement with each other and a slower evaporation in the late stages of gas cycling.

Results for Case 1 are qualitatively the same as for Case 2. Again, companies using precalculated K values found wide differences in the amount of condensate formed and its rate of evaporation compared with companies that used EOS methods. Surprisingly, there was no obvious correlation between the number of components for the heptanes-plus fractions and the predicted rates of evaporation in Node (7,7,4) for the five companies that used EOS methods.

This problem would benefit from PVT data that include some equilibrium flash data for feed compositions that exist in the enrichment zone near the producer. Unfortunately, these data are unavailable and true evaporation rate is unknown at this time. Data of this kind have been measured in previous compositional simulation studies²⁴⁻²⁶ and are needed here to decide which answers are correct.

Reservoir model performance is indicated in Table 29. The nature of IMPES models restricted the timestep size to a value generally less than 30 days, especially in the late stages of cycling as the gas formation factor changes. Machine speed differences were not factored into the comparisons, and only the raw data are given. In-line EOS methods seem to increase run times, but many other factors are involved.

Conclusions

1. Depletion data and lean-gas swelling data for the retrograde gas condensate are matched well by all companies.

2. In early years of cycling with partial pressure maintenance, the surface oil rates disagree by about 20%. Liquid yield in simple pressure depletion (Fig. 4) does not account for this much error. It suggests that differences in pressure caused by physical property errors (Z factors) and/or surface-separator molar split errors may also be responsible.

3. Large discrepancies were observed in incremental oil obtained by gas-sales deferral (Case 2 vs. Case 1); the range was 3 to 8% of initial condensate in place. The median value was 160 MSTB [25.4×10^3 stock-tank m^3], or about 4.5% of the initial condensate.

4. The gas used for recycling in the reservoir model was considerably richer in C_{3+} than the lean gas used for the swelling tests. This was unavoidable because not all companies had gas-plant capability in the reservoir simulator. Nonetheless, it casts doubt on the usefulness of the swelling data for the problem.

5. The pressure range for the swelling data was beyond what is needed for cycling. Several companies chose not to match the high pressure range of the swelling data. This may be valid, but we do not know how it affected results.

6. There is considerable disagreement about condensate saturation in the producing node, Node (7,7,4). This is probably because K values are used as tables or as calculated in line with an EOS. The project does not establish which method gave better answers in this case, but there is more scatter when companies attempt to use K -value tables with no data on which to tune. We were unable to provide these data for this problem.

Acknowledgments

We thank Marathon Oil Co. and Computer Modelling Group for permission to publish this paper and for providing the necessary time and support needed to conduct the project. We thank the participants for their cooperation and well-written responses to the problem. Last, we are indebted to Core Laboratories Inc. for allowing us to use the PVT data essential to this problem.

References

- Odeh, A.S.: "Comparison of Solutions to a Three-Dimensional Black-Oil Simulation Problem," *JPT* (Jan. 1981) 13-25.
- Chappellear, J.E. and Nolen, J.S.: "Second Comparative Project: A Three-Phase Coning Study," *JPT* (March 1986) 345-53.
- Peng, D.Y. and Robinson, D.B.: "A New Two-Constant Equation of State," *Ind. and Eng. Chem. Fund.* (1976) 59-64.
- Lohrenz, J., Bray, B.G., and Clark, C.R.: "Calculating Viscosities of Reservoir Fluids From Their Compositions," *JPT* (Oct. 1964) 1171-76; *Trans.*, AIME, **231**.
- Price, H.S. and Coats, K.H.: "Direct Methods in Reservoir Simulation," *SPEJ* (June 1974) 295-308; *Trans.*, AIME, **257**.
- Reid, R.C., Prausnitz, J.M., and Sherwood, T.K.: *The Properties of Gases and Liquids*, third edition, McGraw-Hill Book Co., New York City (1977) 426.
- Nghiem, L.X., Fong, D.K., and Aziz, K.: "Compositional Modeling With An Equation of State," *SPEJ* (Dec. 1981) **21**, 687-98.
- Nghiem, L.X.: "A New Approach to Quasi-Newton Methods with Application to Compositional Modeling," paper SPE 12242 presented at the 1983 SPE Symposium on Reservoir Simulation, San Francisco, Nov. 15-18.
- Kazemi, H., Vestal, C.R., and Shank, G.D.: "An Efficient Multicomponent Numerical Simulator," *SPEJ* (Oct. 1978) 355-68.
- Coats, K.H. and Smart, G.T.: "Application of a Regression-Based EOS PVT Program to Laboratory Data," paper SPE 11197 presented at the 1982 SPE Annual Technical Conference and Exhibition, New Orleans, Sept. 26-29.
- Whitson, C.H.: "Characterizing Hydrocarbon Plus Fractions," paper EUR 183 presented at the 1980 SPE European Offshore Petroleum Conference, London, Oct. 21-24.
- Coats, K.H.: "An Equation-of-State Compositional Model," *SPEJ* (Oct. 1980) 363-76.
- Meijerink, J.A.: "A New Stabilized Method for Use in IMPES-Type Numerical Reservoir Simulators," paper SPE 5247 presented at the 1974 SPE Annual Technical Conference and Exhibition, Houston, Oct. 6-9.
- Little, J.E. and Kennedy, H.T.: "A Correlation of the Viscosity of Hydrocarbon Systems With Pressure, Temperature and Composition," *SPEJ* (June 1968) 157-62; *Trans.*, AIME, **243**.
- Lee, A.L., Gonzalez, M.H., and Eakin, B.E.: "The Viscosity of Natural Gases," *JPT* (Aug. 1966) 997-1000; *Trans.*, AIME, **237**.
- Watson, K.M., Nelson, E.F., and Murphy, G.B.: "Characterization of Petroleum Fractions," *Ind. and Eng. Chem.* (1935) **27**, 1460-64.

17. Whitson, C.H.: "Effect of C_{7+} Properties on Equation-of-State Predictions," *SPEJ* (Dec. 1984) 685-96.
18. Haaland, S.: "Characterization of North Sea Crude Oils and Petroleum Fractions," MS thesis, Norwegian Inst. of Technol., U. of Trondheim, Norway.
19. Katz, D.L. and Firoozabadi, A.: "Predicting Phase Behavior of Condensate/Crude-Oil Systems Using Methane Interaction Coefficients," *JPT* (Nov. 1978) 1649-55; *Trans.*, AIME, **265**.
20. Kesler, M.G., Lee, B.I., and Sandler, S.I.: "A Third Parameter for Use in General Thermodynamic Correlations," *Ind. and Eng. Chem. Fund.* (1979) **18**, 49-54.
21. Kesler, M.G. and Lee, B.I.: "Improve Prediction of Enthalpy of Fractions," *Hydrocarbon Proc.* (March 1976) 153-58.
22. Stone, H.L.: "Iterative Solution of Implicit Approximations of Multi-Dimensional Partial Differential Equations," *SIAM J. Numer. Anal.* (1968) No. 5, 530-58.
23. "Equation of State Compositional Reservoir Simulator, COMP3, Release 1.2," Scientific Software-Intercomp Corp. (March 3, 1986).
24. Attra, H.D.: "Nonequilibrium Gas Displacement Calculations," *SPEJ* (Sept. 1961) 130-36; *Trans.*, AIME, **222**.
25. Cook, A.B., Walker, C.J., and Spencer, G.B.: "Realistic K Values of C_{7+} Hydrocarbons for Calculating Oil Vaporization During Gas Cycling at High Pressures," *JPT* (July 1969) 901-15; *Trans.*, AIME, **246**.
26. Fussell, D.D. and Yarborough, L.: "The Effect of Phase Data on Liquid Recovery During Cycling of a Gas Condensate Reservoir," *SPEJ* (April 1972) 96-102.

SI Metric Conversion Factors

atm	× 1.013 250*	E+05 = Pa
bbl	× 1.589 873	E-01 = m ³
Btu	× 1.055 056	E+00 = kJ
Btu/ft ³	× 3.725 895	E+01 = kJ/m ³
ft	× 3.048*	E-01 = m
ft ³	× 2.831 685	E-02 = m ³
ft ³ /lbm	× 6.242 796	E+01 = dm ³ /kg
°F	(°F-32)/1.8	= °C
°F	(°F+459.67)/1.8	= K
gal	× 3.785 412	E-03 = m ³
lbm/ft ³	× 1.601 846	E+01 = kg/m ³
psi	× 6.894 757	E+00 = kPa
psi ⁻¹	× 1.450 377	E-01 = kPa ⁻¹
°R	°R/1.8	= K
scf/bbl	× 1.801 175	E-01 = std m ³ /m ³

*Conversion factor is exact.

JPT

Original manuscript received in the Society of Petroleum Engineers office Oct. 24, 1983. Paper accepted for publication Oct. 24, 1986. Revised manuscript received April 23, 1987. Paper (SPE 12278) first presented at the 1983 SPE Reservoir Simulation Symposium held in San Francisco, Nov. 15-18.